EslB is required for cell wall integrity and cell division in *Listeria monocytogenes*

Jeanine Rismondo[a,*,#], Maria Yacoub[a], Ashima Wadhawan[b], Marc S. Dionne[b], Angelika Gründling[a,#]

[a] Section of Molecular Microbiology and Medical Research Council Centre for Molecular Bacteriology and Infection, Imperial College London, London SW7 2AZ.

[b] Department of Life Sciences, Medical Research Council Centre for Molecular Bacteriology and Infection, Imperial College London, London SW7 2AZ.

[*] Present Address: Department of General Microbiology, GZMB, Georg-August-Universität Göttingen, 37077 Göttingen, Germany

[#]To whom correspondence should be addressed:
Jeanine Rismondo – jrismon@gwdg.de, Angelika Gründling – a.grundling@imperial.ac.uk

Running title: Characterization of an *eslB* deletion strain

ABSTRACT

Lysozyme is an enzyme found in secretions including tears, saliva and mucus and is an important component of the innate immune system. It functions by hydrolysing the peptidoglycan layer of bacteria. The human pathogen *Listeria monocytogenes* is intrinsically lysozyme resistant. The peptidoglycan N-deacetylase PgdA and O-acetyltransferase OatA are two known factors contributing to its lysozyme resistance. Furthermore, it was shown that the absence of components of an ABC transporter, here referred to as EslABC, leads to a reduction in lysozyme resistance. However, the function of the transporter and how its activity is linked to lysozyme resistance are still unknown. To investigate this further, a strain with a deletion in *eslB*, coding for the membrane component of the ABC transporter, was constructed in the *L. monocytogenes* strain 10403S. The *eslB* mutant showed as expected a 40-fold reduction in the minimal inhibitory concentration to lysozyme. Using growth and autolysis assays, we further show that the absence of EslB manifests in a growth defect in media containing high concentrations of sugars and increased endogenous cell lysis. However, no growth defect could be detected within host cells. On the other hand, the *eslB* mutant showed slight changes in its peptidoglycan structure as well as a noticeable cell division defect and formed elongated cells. Based on our results, we hypothesize that EslB is important for the maintenance of cell wall integrity in *L. monocytogenes* under specific growth and stress conditions.

IMPORTANCE

The ABC transporter EslABC is associated with the intrinsic lysozyme resistance of *Listeria monocytogenes*. However, the exact role of the transporter in this process and in the physiology of *L. monocytogenes* is unknown. Using different assays to characterize an *eslB* deletion strain, we found that the absence of EslB not only affects lysozyme resistance, but also endogenous autolysis, cell division and the ability of the bacterium to grow in media containing high concentrations of sugars. Our results indicate that EslB is by a yet unknown mechanism an important determinant for cell wall integrity in *L. monocytogenes*.

48 **INTRODUCTION**

49 Gram-positive bacteria are surrounded by a complex cell wall, which is composed of a thick
50 layer of peptidoglycan (PG) and cell wall polymers. The bacterial cell wall is important for the
51 maintenance of cell shape, the ability of bacteria to withstand harsh environmental conditions
52 and to prevent cell lysis (Höltje, 1998, van Heijenoort, 2001). Due to its importance, cell wall-
53 targeting antibiotics such as β-lactam, glycopeptide, fosfomycin and moenomycin antibiotics
54 are commonly used to treat bacterial infections (Koch, 2003, Sarkar et al., 2017). These cell-
55 wall targeting antibiotics inhibit enzymes involved in different stages of the PG biosynthesis
56 process (Sarkar et al., 2017). Moenomycin and β-lactam antibiotics, for instance, block the
57 glycosyltransferase and transpeptidase activity of penicillin binding proteins, respectively,
58 which are required for the polymerization and crosslinking of the glycan strands (Huber and
59 Nesemann, 1968, Sauvage and Terrak, 2016, Tipper and Strominger, 1965). Peptidoglycan is
60 also the target of the cell wall hydrolase lysozyme, which is a component of animal and human
61 secretions such as tears and mucus. Lysozyme cleaves the glycan strands of PG by hydrolysing
62 the 1,4-β-linkage between N-acetylmuramic acid (MurNAc) and N-acetylglucosamine
63 (GlcNAc). This reaction leads to a loss of cell integrity and results in cell lysis (Callewaert and
64 Michiels, 2010). The intracellular human pathogen *Listeria monocytogenes* is intrinsically
65 resistant to lysozyme due to modifications of its PG. The N-deacetylase PgdA deacetylates
66 GlcNAc residues, whereas MurNAc residues are acetylated by the O-acetyltransferase OatA
67 (Boneca et al., 2007, Aubry et al., 2011). Consequently, deletion of either of these enzymes
68 results in reduced lysozyme resistance (Boneca et al., 2007, Aubry et al., 2011). One or both
69 of these enzymes are also present in other bacterial pathogens and important for lysozyme
70 resistance, such as for instance PgdA in *Streptococcus pneumoniae,* OatA in *Staphylococcus*
71 *aureus* and PgdA and OatA in *Enterococcus faecalis* (Benachour et al., 2012, Hébert et al.,
72 2007, Vollmer and Tomasz, 2000, Bera et al., 2005). Besides enzymes that directly alter the
73 peptidoglycan structure, a number of other factors have been shown to contribute to lysozyme
74 resistance in diverse bacteria. For instance, the cell wall polymer wall teichoic acid and the
75 two-component system GraRS contribute to lysozyme resistance in *S. aureus* (Bera et al., 2007,
76 Herbert et al., 2007). In *E. faecalis*, the extracytoplasmic function sigma factor SigV is required
77 for the upregulation of *pgdA* expression in the presence of lysozyme (Le Jeune et al., 2010,
78 Benachour et al., 2012). Recently, other factors have also been identified, which contribute to
79 the intrinsic lysozyme resistance of *L. monocytogenes* such as the predicted carboxypeptidase
80 PbpX, the transcription factor DegU and the noncoding RNA Rli31 (Burke et al., 2014). DegU
81 and Rli31 are involved in the regulation of *pgdA* and *pbpX* expression in *L. monocytogenes*

82 (Burke et al., 2014). Furthermore, components of a predicted ABC transporter encoded by the
83 *lmo2769-6* operon in *L. monocytogenes* and here referred to as *eslABCR* for elongation, sugar-
84 and lysozyme sensitive phenotype (Fig. 1), have been associated with lysozyme resistance
85 (Burke et al., 2014, Durack et al., 2015, Toledo-Arana et al., 2009). An *eslB* mutant strain was
86 also shown to be more sensitive to cefuroxime and cationic antimicrobial peptides (Burke et
87 al., 2014).
88 ABC transporters can either act as importers or exporters. Importers are involved in the
89 uptake of sugars, peptides or other metabolites, which are recognized by substrate binding
90 proteins. On the other hand, toxic compounds such as antibiotics can be exported by ABC
91 exporters (Higgins, 1992, Berntsson et al., 2010, Tanaka et al., 2018). ABC transporters are
92 usually composed of homo- or heterodimeric cytoplasmic nucleotide-binding domain (NBD)
93 proteins, also referred to as ATP-binding cassette proteins, and homo- or heterodimeric
94 transmembrane domain (TMD) proteins (Locher, 2016). In ABC exporters belonging to the B-
95 family, such as the *S. aureus* multidrug transporter Sav1866, NBDs and TMDs are fused
96 (Dawson and Locher, 2006, Locher, 2016). Other ABC transporters, e.g. type I and type II
97 ABC importers, consist of a complex of heterodimers of NBD- and TMD-containing proteins
98 (Locher, 2016). In addition to NBDs and TMDs, type I and type II ABC importers have an
99 extracellular substrate binding protein (SBP), which is important for the delivery of specific
100 substrate molecules to the transporter (Davidson et al., 2008). Type III or energy-coupling
101 factor (ECF) transporters use a membrane-integrated S component for substrate-binding
102 (Mächtel et al., 2019, Slotboom, 2014). The *esl* operon encodes EslA, the NBD protein, EslB,
103 the TMD protein forming part of the ABC transporter, EslC, a membrane protein of unknown
104 function and EslR, the RpiR-type transcriptional regulator (Fig. 1). So far, it is not known
105 whether the predicted ABC transporter EslABC acts as an importer or exporter and its exact
106 cellular function has not been identified. Furthermore, it has not been investigated whether
107 EslC is a component of the ABC transporter encoded in the *esl* operon, e.g. a protein similar to
108 the S component of the ECF transporters, or whether it functions independent from EslAB.
109 Here, we show that the absence of EslB, the transmembrane part of the ABC transporter, not
110 only leads to an increased lysozyme sensitivity, but also to an increased endogenous cell lysis
111 and a cell division defect. We hypothesize that EslB may be required for the maintenance of
112 the cell wall integrity of *L. monocytogenes* during stress conditions.
113
114
115

116 **MATERIALS AND METHODS**

117 **Bacterial strains and growth conditions.** All strains and plasmids used in this study are listed
118 in Table S1. *Escherichia coli* strains were grown in Luria-Bertani (LB) medium and *Listeria*
119 *monocytogenes* strains in brain heart infusion (BHI) medium at 37°C unless otherwise stated.
120 If necessary, antibiotics and supplements were added to the medium at the following
121 concentrations: for *E. coli* cultures, ampicillin (Amp) at 100 µg/ml, chloramphenicol (Cam) at
122 20 µg/ml and kanamycin (Kan) at 30 µg/ml, and for *L. monocytogenes* cultures, Cam at 10
123 µg/ml, erythromycin (Erm) at 5 µg/ml, Kan at 30 µg/ml and IPTG at 1 mM.
124

125 **Strain and plasmid construction.** All primers used in this study are listed in Table S2. For
126 the markerless inframe deletion of *lmo2768* (*lmrg_01927*, *eslB*), approximately 1kb-DNA
127 fragments up- and downstream of the *eslB* gene were amplified by PCR using primer pairs
128 ANG2532/2533 and ANG2534/2535. The resulting PCR products were fused in a second PCR
129 using primers ANG2532/2535, the product was cut with BamHI and XbaI and ligated with
130 plasmid pKSV7 that had been cut with the same enzymes. The resulting plasmid pKSV7-Δ*eslB*
131 was recovered in *E. coli* XL1-Blue yielding strain ANG4236. The plasmid was subsequently
132 transformed into *L. monocytogenes* strain 10403S and *eslB* deleted by allelic exchange using a
133 previously described procedure (Camilli et al., 1993). The deletion of *eslB* was verified by
134 PCR. The deletion procedure was performed with two independent transformants and resulted
135 in the construction of two independent *eslB* mutant strains 10403SΔ$eslB_{(1)}$ (ANG4275) and
136 10403SΔ$eslB_{(2)}$ (ANG5662). For complementation analysis, pIMK3-*eslB* was constructed, in
137 which the expression of *eslB* can be induced by IPTG. The gene *eslB* was amplified using
138 primer pair ANG2812/ANG2813, cut with NcoI and SalI and fused with pIMK3 that had been
139 cut with the same enzymes. The resulting plasmid pIMK3-*eslB* was recovered in *E. coli* XL1-
140 Blue yielding strain ANG4647. Due to difficulties in preparing electrocompetent cells of *L.*
141 *monocytogenes eslB* mutant strains, plasmid pIMK3-*eslB* was first electroporated into the
142 wildtype *L. monocytogenes* strain 10403S yielding strain 10403S pIMK3-*eslB* (ANG4678). In
143 the second step, *eslB* was deleted from the genome of strain ANG4678 resulting in the
144 construction of the first *eslB* complementation strain 10403SΔ$eslB_{(1)}$ pIMK3-*eslB* (ANG4688,
145 short 10403SΔ$eslB_{(1)}$ compl.). In addition, complementation plasmid pPL3e-P_{eslA}-*eslABC* was
146 constructed. To this end, the *eslABC* genes including the upstream promoter region were
147 amplified by PCR using primers ANG3349/ANG3350. The resulting PCR product was cut
148 with SalI and BamHI and fused with plasmid pPL3e that had been cut with the same enzymes.

149 Plasmid pPL3e-P$_{eslA}$-*eslABC* was recovered in *E. coli* XL1-Blue yielding strain ANG5660.
150 Next, plasmid pPL3e-P$_{eslA}$-*eslABC* was transformed into *E. coli* SM10 yielding strain
151 ANG5661. Lastly, SM10 pPL3e-P$_{eslA}$-*eslABC* was used as a donor strain to transfer plasmid
152 pPL3e-P$_{eslA}$-*eslABC* by conjugated into *L. monocytogenes* strain 10403SΔ*eslB*$_{(2)}$ (ANG5662)
153 using a previously described method (Lauer et al., 2002). This resulted in the construction of
154 the second *eslB* complementation strain 10403SΔ*eslB*$_{(2)}$ pPL3e-P$_{eslA}$-*eslABC* (ANG5663, short
155 10403SΔ*eslB*$_{(2)}$ compl.).
156
157 **Whole genome sequencing.** Genomic DNA of *L. monocytogenes* was extracted using the
158 FastDNA™ Kit (MP Biomedicals) and libraries for sequencing prepared using the Illumina
159 Nextera DNA kit. The samples were sequenced at the London Institute of Medical Sciences
160 using an Illumina MiSeq machine and a 150 paired end Illumina kit. The reads were trimmed,
161 mapped to the *L. monocytogenes* 10403S reference genome (NC_017544) and single
162 nucleotide polymorphisms (SNPs) with a frequency of at least 80% and small deletions (zero
163 coverage) identified using CLC workbench genomics (Qiagen).
164
165 **Growth analysis.** *L. monocytogenes* strains were grown overnight in 5 ml BHI medium at
166 37°C with shaking. The next day, these cultures were used to inoculate 15 ml fresh BHI
167 medium or BHI medium containing 0.5 M sucrose, fructose, glucose, maltose, galactose or
168 sodium chloride to an OD_{600} of 0.05. The cultures were incubated at 37°C with shaking at 180
169 rpm, OD_{600} readings were taken every hour for 8 h. Averages values and standard deviations
170 from three independent experiments were plotted.
171
172 **Fluorescence and phase contrast microscopy.** Overnight cultures of the indicated *L.*
173 *monocytogenes* strains were diluted 1:100 in BHI medium and grown for 3 h at 37°C. For
174 staining of the bacterial membrane, 100 µl of these cultures were mixed with 5 µl of 100 µg/ml
175 nile red solution and incubated for 20 min at 37°C. The cells were washed twice with PBS and
176 subsequently suspended in 50 µl of PBS. 1-1.5 µl of the different samples were subsequently
177 spotted on microscope slides covered with a thin agarose film (1.5 % agarose in distilled water),
178 air-dried and covered with a cover slip. Phase contrast and fluorescence images were taken at
179 1000x magnification using the Zeiss Axio Imager.A1 microscope coupled to the AxioCam
180 MRm and processed using the Zen 2012 software (blue edition). The nile red fluorescence
181 signal was detected using the Zeiss filter set 00. The length of 300 cells was measured for each

182 experiment and the median cell length was calculated. Averages values and standard deviations
183 of the median cell length of three independent experiments were plotted.
184
185 **Determination of minimal inhibitory concentration (MIC).** The minimal inhibitory
186 concentration for the cell wall-acting antibiotics penicillin and moenomycin and the cell wall
187 hydrolase lysozyme was determined in 96-well plates using a microbroth dilution assay.
188 Approximately 10^4 *L. monocytogenes* cells were used to inoculate 200 µl BHI containing two-
189 fold dilutions of the different antimicrobials. The starting antibiotic concentrations were: 0.025
190 µg/ml for penicillin G, 0.2 µg/ml moenomycin and 10 mg/ml or 0.25 mg/ml for lysozyme. The
191 96-well plates were incubated at 37°C with shaking at 500 rpm in a plate incubator
192 (Thermostar, BMG Labtech) and OD_{600} determined after 24 hours of incubation. The MIC
193 value refers to the antibiotic concentration at which bacterial growth was inhibited by >90%.
194
195 **Peptidoglycan isolation and analysis.** Overnight cultures of 10403SΔ*eslB*$_{(1)}$ and
196 10403SΔ*eslB*$_{(1)}$ compl. were diluted in 1 L BHI broth (supplemented with 1 mM IPTG for
197 strain 10403SΔ*eslB*$_{(1)}$ compl.) to an OD_{600} of 0.06 and incubated at 37°C. At an OD_{600} of 1,
198 bacterial cultures were cooled on ice for 1h and the bacteria subsequently collected by
199 centrifugation. The peptidoglycan was purified, digested with mutanolysin and the
200 muropeptides analyzed by HPLC using an Agilent 1260 infinity system, as previously
201 described (de Jonge et al., 1992, Corrigan et al., 2011). Peptidoglycan of the wildtype *L.*
202 *monocytogenes* strain 10403S was purified and analyzed in parallel. The chromatogram of the
203 same wild-type control strain was recently published (Rismondo et al., 2019) and also used as
204 part of this study, since all strains were analyzed at the same time. The major peaks 1-6 were
205 assigned according to previously published HPLC spectra (Burke et al., 2014, Rismondo et al.,
206 2015), with peaks 2, 4, 5 and 6 corresponding to N-deacetylated GlcNAc residues. Peaks 1-2
207 correspond to monomeric and peaks 4-6 to dimeric (crosslinked) muropeptide fragments. The
208 Agilent Technology ChemStation software was used to integrate the areas of the main
209 muropeptide. For quantification, the sum of the peak areas was set to 100% and the area of
210 individual peaks was determined. The sum of values for peaks 3-6 corresponds to the %
211 crosslinking, whereas the deacetylation state was calculated by adding up the values for peaks
212 4, 5 and 6. Averages values and standard deviations were calculated from three independent
213 extractions.
214

215 **Autolysis assays.** *L. monocytogenes* strains were diluted in BHI or BHI medium supplemented
216 with 0.5 M sucrose to an OD_{600} of 0.05 and grown for 4 h at 37°C. Cells were collected by
217 centrifugation and resuspended in 50 mM Tris-HCl, pH 8 to an OD_{600} of 0.7-0.9 and incubated
218 at 37°C. For penicillin- and lysozyme-induced lysis, 25 µg/ml penicillin G or 2.5 µg/ml
219 lysozyme was added to the cultures. Autolysis was followed by determining OD_{600} readings
220 every 15 min.
221
222 **Cell culture.** Bone marrow-derived macrophages (BMMs) were extracted from female
223 C57BL/6 mice as described previously (Stapels et al., 2018). BMMs were a gift from Charlotte
224 S. C. Michaux and Sophie Helaine. $5x10^5$ BMMs were seeded into each well of a 24-well plate
225 and grown overnight in 500 µl high glucose Dulbecco's Modified Eagle Medium (DMEM) at
226 37°C and 5% CO_2. *L. monocytogenes* strains were grown overnight without shaking in 2 ml
227 BHI medium at 30°C. The next morning, bacteria were opsonized with 8% mouse serum
228 (Sigma) at room temperature for 20 min and BMMs were infected for one hour at a multiplicity
229 of infection (MOI) of 2. BMMs were washed with PBS and 1 ml DMEM containing 40 µg/ml
230 gentamycin was added to kill extracellular bacteria. After 1 h, cells were washed with PBS and
231 covered with 1 ml DMEM containing 10 µg/ml gentamycin. The number of recovered bacteria
232 was determined 2, 4, 6 and 8 h post infection. To this end, BMMs were lysed using 1 ml PBS
233 containing 0.1% (v/v) triton X-100 and serial dilutions were plated on BHI agar plates. The
234 number of colony forming units (CFUs) was determined after incubating the plates overnight
235 at 37°C. Three technical repeats were performed for each experiment and average values
236 calculated. Average values and standard deviations from three independent experiments were
237 plotted.
238
239 ***Drosophila melanogaster* infections.** Fly injections were carried out with microinjection
240 needles produced from borosilicate glass capillaries (World Precision Instruments TW100-4)
241 and a needle puller (Model PC-10, Narishige). Injections were performed using a Picospritzer
242 III system (Parker Hannifin), and the injection volume was calibrated by expelling a drop of
243 liquid from the needle into a pot of mineral oil and halocarbon oil (both Sigma). The expelled
244 drop was measured using the microscope graticule to obtain a final injection volume of 50
245 nanolitres (nl). Flies were then anesthetized with CO_2 and injected with either 50 nl of bacterial
246 suspension in PBS or sterile PBS. 5-7-day old age matched male flies were used for all
247 experiments. Flies were grouped into uninjected control, wounding control (injection with
248 sterile PBS), and flies infected with *L. monocytogenes*. Each group consisted of 58-60 flies.

249 All survival experiments were conducted at 29°C. Dead flies were counted daily. Food vials
250 were placed horizontally to reduce the possibility of fly death from flies getting stuck to the
251 food, and flies were transferred to fresh food every 3-4 days. For the quantification of the
252 bacterial load, 16 flies per condition and per bacterial strain were collected at the indicated time
253 points. The flies were homogenised in 100 µl of TE-buffer pH 8 containing 1% Triton X-100
254 and 1% Proteinase K (NEB, P8107S). Homogenates were incubated for 3 h at 55°C followed
255 by a 10 min incubation step at 95°C. Following incubation, qPCR was carried out using the
256 *actA* gene specific primers EGD-E_ActA_L1 and EGD-E_ActA_R1 to determine the number
257 of bacterial colony forming units. PCR was performed with Sensimix SYBR Green no-ROX
258 (Bioline) on a Corbett Rotor-Gene 6000. The cycling conditions were as follows: Hold 95°C
259 for 10 min, then 45 cycles of 95°C for 15 s, 57°C for 30 s, 72°C for 30 s, followed by a melting
260 curve. Gene abundances were calculated as previously described (Sharrock et al., 2019).
261

262 **RESULTS**

263 **Deletion of *eslB* in *L. monocytogenes* leads to lysozyme resistance and a slight increase in**
264 **peptidoglycan crosslinking.**

265 Previously it has been shown that *L. monocytogenes* strains with mutations in the *eslABCR*
266 operon (Fig. 1A) display decreased resistance towards the cell wall hydrolase lysozyme (Burke
267 et al., 2014, Durack et al., 2015). The *eslABC* operon codes for a predicted ABC transporter,
268 however, the function of this transporter and how its activity is linked to lysozyme resistance
269 are still unknown. To investigate this further, a strain with a markerless in-frame deletion in
270 *eslB,* coding for the membrane component of the ABC transporter, was constructed in the *L.*
271 *monocytogenes* strain 10403S. Confirming previous results, the *eslB* deletion strain had a 40-
272 fold lower MIC for lysozyme as compared to the wildtype strain (Fig. 2A) (Durack et al., 2015,
273 Burke et al., 2014). This phenotype could be complemented and strain 10403SΔ*eslB*$_{(1)}$ compl.,
274 in which *eslB* is expressed from an IPTG-inducible promoter, is even slightly more resistant to
275 lysozyme as compared to the wildtype strain (Fig. 2A). Next, we tested whether the resistance
276 towards two other cell wall-targeting antibiotics, namely penicillin and moenomycin, is
277 changed upon deletion of *eslB*. The MIC values obtained for the wildtype, *eslB* deletion and
278 *eslB* complementation strains were comparable (Fig. 2B-C), suggesting that the deletion of
279 *eslB* does not lead to a general sensitivity to all cell wall-acting antimicrobials but is specific
280 to lysozyme. In *L. monocytogenes*, lysozyme resistance is achieved by the modification of the
281 peptidoglycan (PG) by N-deacetylation via PgdA and O-acetylation via OatA (Boneca et al.,

282 2007, Aubry et al., 2011). To assess whether deletion of *eslB* impacts the N-deacetylation and
283 crosslinking of PG, PG was isolated from wildtype 10403S, the *eslB* deletion and
284 complementation strains, digested with mutanolysin and the muropeptides analysed by high
285 performance liquid chromatography (HPLC). This analysis revealed a slight increase in the PG
286 crosslinking in the *eslB* mutant strain (68±0.53%) compared to the wildtype (65.47±0.31%)
287 and the complementation strain grown in the presence of IPTG (64.57±2.3%) (Fig. 3). The PG
288 isolated from the *eslB* deletion strain was also slightly more deacetylated (71.54±0.21%) as
289 compared to the wildtype (67.17±0.31%) and the complementation strain (67±2.27%) (Fig. 3),
290 which should theoretically result in an increase and not decrease in lysozyme resistance. Taken
291 together, while slight changes in the PG structure were observed in the *eslB* mutant strain, our
292 results suggest that the lysozyme sensitivity of the *eslB* deletion strain is not caused by a defect
293 in PgdA enzyme activity and increased N-acetylation of GlcNAc residues.
294
295 **Deletion of *eslB* results in increased endogenous and lysozyme-induced lysis.**
296 The observed lysozyme sensitivity of the *eslB* deletion strain could also be a result of an
297 increased autolysis due to an impaired cell integrity. To test this, autolysis assays were
298 performed. To this end, the *L. monocytogenes* wildtype strain 10403S, the *eslB* deletion and
299 complementation strains were grown for 4 h in BHI medium, bacteria collected by
300 centrifugation and suspended in 50 mM Tris-HCl buffer (pH 8). After 2 h incubation at 37°C,
301 the OD_{600} of the suspensions of the wildtype and *eslB* complementation strain had dropped to
302 89.9±1.6% and 86.5±2.9% of the initial OD_{600}, respectively. (Fig. 4A). Enhanced endogenous
303 cell lysis was observed for the *eslB* mutant strain and the OD_{600} of the suspensions had dropped
304 to 68.8±1.7% (Fig. 4A). Interestingly, the addition of penicillin had no impact on the autolysis
305 rate of any of the strains tested (Fig. 4B). On the other hand, the addition of 2.5 µg/ml lysozyme
306 increased the autolysis rate of all strains, but had a particularly drastic effect on the *eslB* mutant
307 strain. After 30 min, the OD_{600} reading of a suspension of the *eslB* deletion strain had dropped
308 to 50.3±10.2%. For the wildtype and *eslB* complementation strains, it took 90 min to see a 50%
309 reduction in OD_{600} readings of the suspensions (Fig. 4B). These results show that the absence
310 of EslB leads to an increased endogenous autolysis of *L. monocytogenes* cells that can be
311 further enhanced by the addition of lysozyme.
312
313
314

315 **Deletion of *eslB* results in a growth defect in high sugar media.**
316 The bacterial cell wall is an important structure to maintain the cell integrity and to prevent
317 lysis due to the high internal turgor pressure or when bacteria experience changes in the
318 external osmolality. Cell wall defects leading to an impaired cell integrity could affect the
319 growth of bacteria in environments with high osmolalities, e.g. in the presence of high salt or
320 sugar concentrations. Next, we compared the growth of the wildtype, the *eslB* mutant and
321 complementation strains at 37°C in different media. No growth difference could be observed
322 between the strains tested, when grown in BHI medium (Fig. 5A). However, the *eslB* deletion
323 strain grew slower in BHI medium containing 0.5 M sucrose as compared to the wildtype and
324 the *eslB* complementation strain (Fig. 5B). A similar growth phenotype could be observed
325 when the strains were grown in BHI medium containing either 0.5 M fructose, glucose, maltose
326 or galactose (Fig. S1). In contrast, the presence of 0.5 M NaCl did not affect the growth of the
327 *eslB* deletion strain (Fig. 5C). These results suggest that the observed growth defect seen for
328 the *eslB* mutant is not solely caused by the increase in external osmolality, but rather seems to
329 be specific to the presence of high concentrations of sugars.
330 Next, we wanted to determine which impact the growth in the presence of high levels of sucrose
331 has on endogenous bacterial autolysis rates. To this end, the wildtype 10403S, *eslB* mutant and
332 complementation strains were grown in BHI medium supplemented with 0.5 M sucrose, cell
333 suspensions prepared in Tris-buffer and used in autolysis assays. While the wildtype and
334 complementation strain showed similar autolysis rates following growth in BHI sucrose
335 medium (Fig. 6A) as after growth in BHI medium (Fig 4A), the *eslB* mutant that had been
336 transferred into Tris-buffer after growth in BHI 0.5 M sucrose medium lysed rapidly (Fig. 6A).
337 The lysis of the *eslB* mutant strain could be further enhanced by the addition of 25 µg/ml
338 penicillin, a concentration which only acts bacteriostatic on the *L. monocytogenes* wildtype
339 strain 10403S (Fig. 6B). These findings strengthen the hypothesis that the absence of EslB
340 results in an impaired cell wall integrity.
341
342 **The *eslB* deletion strain is impaired in cell division, but not in virulence.**
343 The increased endogenous autolysis together with the observed changes in the PG structure of
344 the *eslB* deletion strain could result in an increased sensitivity to autolysins. The major
345 autolysins of *L. monocytogenes* are p60 and NamA (MurA), which hydrolyze PG and are
346 required for daughter cell separation during cell division (Pilgrim et al., 2003, Carroll et al.,
347 2003). Absence of either p60 or NamA results in the formation of cell chains (Carroll et al.,
348 2003, Pilgrim et al., 2003). We thus wondered whether deletion of *eslB* causes changes in the

349 cell morphology in *L. monocytogenes*. Microscopic analysis revealed that cells lacking EslB
350 are significantly longer with a median cell length of 3.36±0.49 µm as compared to the *L.*
351 *monocytogenes* wildtype strain, which produced cells with a length of 1.91±0.02 µm (Fig. 7),
352 highlighting that the absence of EslB therefore results in a cell division defect.
353 Next, we wanted to assess whether the impaired cell integrity and the observed cell division
354 defect would also affect the virulence of the *L. monocytogenes eslB* mutant. Of note, in a
355 previous study, it was shown that deletion of *eslA*, coding for the ATP-binding protein
356 component of the ABC transporter, has no effect on the cell-to-cell spread of *L. monocytogenes*
357 (Durack et al., 2015). Before assessing the contribution of EslB to the virulence potential of *L.*
358 *monocytogenes,* we wanted to ensure that the *eslB* mutant we constructed did not contain any
359 other genomic alteration that could impact the pathogenicity of this strain. Our whole genome
360 sequencing (WGS) analysis revealed that strain 10403SΔ*eslB*$_{(1)}$ contained an additional small
361 deletion in gene *lmo2396* coding for an internalin protein with a leucine-rich repeat (LRR) and
362 a mucin-binding domain (Table S3). While to the best of our knowledge, the contribution of
363 Lmo2396 to the pathogenicity of *L. monocytogenes* has not yet been investigated, other
364 internalins are important and well-established virulence factors (Gaillard et al., 1991, Bierne et
365 al., 2007) and hence our original *eslB* mutant strain 10403SΔ*eslB*$_{(1)}$ might not be ideal to
366 investigate the contribution of EslB to the virulence potential of *L. monocytogenes*. Our WGS
367 analysis also revealed a single point mutation in gene *lmo2342*, coding for a pseudouridylate
368 synthase in the complementation strain 10403SΔ*eslB*$_{(1)}$ compl. (Table S3). Since we identified
369 an additional mutation in a gene coding for a potential virulence factor in our first *eslB* mutant
370 strain, we constructed a second independent *eslB* mutant, 10403SΔ*eslB*$_{(2)}$. We also constructed
371 a second complementation strain, strain 10403SΔ*eslB*$_{(2)}$ p*PeslA-eslABC* (or short
372 10403SΔ*eslB*$_{(2)}$ compl.), in which the *eslABC* genes are expressed from the native *eslA*
373 promoter from a chromosomally integrated plasmid. Our WGS analysis revealed that strain
374 10403SΔ*eslB*$_{(2)}$ did not contain any secondary mutations (Table S3). A 1-bp deletion in gene
375 *lmo2022* encoding a predicted NifS-like protein required for NAD biosynthesis, was identified
376 in strain 10403SΔ*eslB*$_{(2)}$ compl. (Table S3), which if non-complementable phenotypes are
377 observed needs to be kept in mind.
378 Next, we confirmed that our second *eslB* mutant strain 10403SΔ*eslB*$_{(2)}$, which does not contain
379 any additional chromosomal mutations, showed the same lysozyme sensitivity, growth defect
380 in BHI sucrose medium and formed elongated cells as our original *eslB* mutant strain
381 10403SΔ*eslB*$_{(1)}$ (Fig. S2). Furthermore, all phenotypes could be reverted back to wildtype

382 levels in our newly constructed complementation strain 10403SΔ*eslB*$_{(2)}$ compl., in which *eslB*
383 is expressed along with *eslA and eslC* from their proceeding native promoter (Fig. S2).
384 To determine whether EslB is involved in the virulence of *L. monocytogenes*, primary mouse
385 macrophages were infected with wildtype 10403S, the *eslB* mutant 10403SΔ*eslB*$_{(2)}$ and
386 complementation strain 10403SΔ*eslB*$_{(2)}$ compl.. All three strains showed a comparable
387 intracellular growth pattern (Fig. 8A), suggesting that EslB does not impact the ability of *L.*
388 *monocytogenes* to grow in primary mouse macrophages. Next, we assessed the ability of the
389 *eslB* deletion strains to kill *Drosophila melanogaster* as lysozyme is one important component
390 of its innate immune response (Daffre et al., 1994). All uninfected flies (U/C) and 96.6% of
391 the flies that were injected with PBS survived the duration of the experiment (Fig. 8B). Flies
392 infected with strains 10403SΔ*eslB*$_{(1)}$ and 10403SΔ*eslB*$_{(2)}$ showed an increase in survival in
393 comparison to the wildtype strain. However, these differences were not statistically significant
394 (Fig. 8B). In addition, the difference in killing by the 10403SΔ*eslB*$_{(2)}$ could not be
395 complemented by the expression of *eslABC* in strain 10403SΔ*eslB*$_{(2)}$ compl. (Fig. 8B). Finally,
396 no statistically significant differences could be observed for the bacterial load of flies infected
397 with the different *L. monocytogenes* strains (Fig. 8C). These results indicate that, while EslB
398 does not impact the ability of *L. monocytogenes* to infect and kill mammalian macrophages or
399 *Drosophila melanogaster*, it nonetheless impacts the cell division and cell wall integrity of *L.*
400 *monocytogenes* by a yet unknown mechanism.
401
402 **DISCUSSION**
403 Over the past years, several determinants contributing to the intrinsic lysozyme resistance of
404 *L. monocytogenes* have been described (Boneca et al., 2007, Aubry et al., 2011, Burke et al.,
405 2014, Durack et al., 2015). One of these is a predicted ABC transporter encoded as part of the
406 *eslABCR* operon (Burke et al., 2014, Durack et al., 2015). In this study, we aimed to further
407 investigate the role of the ABC transporter EslABC in *L. monocytogenes* by constructing and
408 characterizing an *eslB* deletion strain, which also in our hands showed a significant increase in
409 lysozyme sensitivity. We further found that the PG isolated from the *eslB* mutant was slightly
410 more crosslinked and also the fraction of deacetylated GlcNAc residues was slightly increased
411 as compared to the PG isolated from the wildtype strain 10403S. Deacetylation of GlcNAc
412 residues in PG is achieved by the N-deacetylase PgdA and has been shown to lead to increased
413 lysozyme resistance (Boneca et al., 2007). Since we saw a slight increase in the deacetylation
414 of GlcNAc residues in the *eslB* mutant strain, our results indicate that the lysozyme sensitivity

415 phenotype of the *eslB* deletion strain is independent of PgdA and that this enzyme functions
416 properly in the mutant strain. Lysozyme also acts as a cationic antimicrobial peptide (CAMP),
417 which permeabilizes the bacterial membrane (Herbert et al., 2007, Ibrahim et al., 2002). Cells
418 lacking EslB might therefore be more susceptible to this non-enzymatic activity of lysozyme.
419 Indeed, a previous study showed that disruption of *eslB* affects the resistance to CAMPs (Burke
420 et al., 2014). Another possible explanation for the increased lysozyme sensitivity of the *eslB*
421 deletion strain could be an impaired cell wall integrity, perhaps specifically at the cell division
422 site. Absence of EslB leads to the formation of elongated cells, however, it is currently not
423 clear how the function of EslABC is linked to cell division of *L. monocytogenes*. EslABC could
424 potentially affect the localization of cell division-specific proteins and deletion of *eslB* could
425 lead to a delayed assembly of the divisome, which could lead to an altered PG biosynthesis at
426 the division site and an impaired cell integrity. Indeed, cells of the *eslB* mutant lysed more
427 rapidly as compared to the *L. monocytogenes* wildtype strain 10403S when shifted from BHI
428 broth to Tris-buffer. The autolysis of cells lacking EslB was strongly induced following growth
429 in BHI supplemented with 0.5 M sucrose prior to the incubation in Tris-buffer. These results
430 indicate that the *eslB* mutant is sensitive to an osmotic downshift and we hypothesize that this
431 is due to an impaired cell integrity.
432 Growth comparisons in different media also revealed that the absence of EslB results in a
433 reduced growth in BHI broth containing high concentrations of mono- or disaccharides. One
434 could speculate that the EslABC transporter might be a sugar transporter with a broad sugar
435 spectrum. The genomic locus of *eslB* supports this hypothesis as the *eslABC* genes are co-
436 transcribed with *eslR* coding for a RpiR family transcriptional regulator (Toledo-Arana et al.,
437 2009). Members of the RpiR transcriptional regulators family are usually involved in the
438 control of sugar phosphate metabolic pathways (Sorensen and Hove-Jensen, 1996, Jaeger and
439 Mayer, 2008, Poulsen et al., 1999, Kim et al., 1997, Yamamoto et al., 2001). The RpiR
440 regulator MurR regulates the MurNAc etherase MurQ in *Escherichia coli* that is essential for
441 the catabolism of MurNAc, a component of the bacterial cell wall (Jaeger and Mayer, 2008).
442 *murQ* is transcribed in an operon with *murP*, coding for a MurNAc-specific EIIBC of the
443 phosphotransferase system (PTS), which is responsible for the import of MurNAc from the
444 growth medium (Dahl et al., 2004). This links the import of sugars by a PTS transporter, whose
445 activity is regulated by the RpiR family transcription factor MurR, with the cell wall
446 biosynthesis in *E. coli*. Accordingly, the transport of sugars by EslABC could therefore impact
447 processes involved in cell wall biosynthesis and the maintenance of cell integrity. Future
448 studies will aim to investigate this further.

449 A reduction in lysozyme resistance is often associated with reduced virulence. An *E. faecalis*
450 strain with a deletion in the gene coding for the peptidoglycan deacetylase PgdA, showed a
451 reduced ability to kill *Galleria mellonella* (Benachour et al., 2012). Similarly, a *S. pneumoniae*
452 *pgdA* mutant showed a decreased virulence in a mouse model of infection (Vollmer and
453 Tomasz, 2000). In our study, we found that inactivation of EslB does not affect the intracellular
454 growth of *L. monocytogenes* in primary mouse macrophages or the ability to kill *Drosophila*
455 *melanogaster*. These observations are consistent with a previous report that another component
456 of the EslABC transporter, EslA, is dispensable for the ability of *L. monocytogenes* to spread
457 from cell to cell (Durack et al., 2015). Previously, it was also shown that combined inactivation
458 of PgdA and OatA reduced the ability of *L. monocytogenes* to grow in bone-marrow derived
459 macrophages, whereas inactivation of PgdA alone had no impact on the virulence of *L.*
460 *monocytogenes* (Rae et al., 2011). We therefore reason that the reduction in lysozyme
461 resistance upon deletion of *eslB* is not strong enough to affect the ability of *L. monocytogenes*
462 to grow and survive in primary macrophages and flies.
463 Taken together, we could show that EslB is not only important for the resistance towards
464 lysozyme, its absence also affects the autolysis, cell division and ability of *L. monocytogenes*
465 to grow in media containing high concentrations of sugars. We hypothesize that the function
466 of the ABC transporter EslABC is directly or indirectly linked to processes involved in the cell
467 wall biosynthesis and maintenance of cell integrity in *L. monocytogenes*.
468
469
470 **ACKNOWLEDGEMENTS**
471 We thank Ivan Andrew and Jaspreet Haywood from the CSC Genomics Laboratory,
472 Hammersmith Hospital, for their help with the whole genome sequencing and Annika Gillis
473 for help with the genome sequence analysis. We would also like to thank Charlotte S. C.
474 Michaux and Sophie Helaine for the bone marrow-derived macrophages. This work was
475 funded by the Wellcome Trust grant 210671/Z/18/Z and MRC grant MR/P011071/1 to AG,
476 the German research foundation (DFG) grant RI 2920/1-1 to JR, and the Wellcome Trust grant
477 207467/Z/17/Z and MRC grant MR/R00997X/1 to MSD.
478

479 **FIGURES AND FIGURE LEGENDS**

480

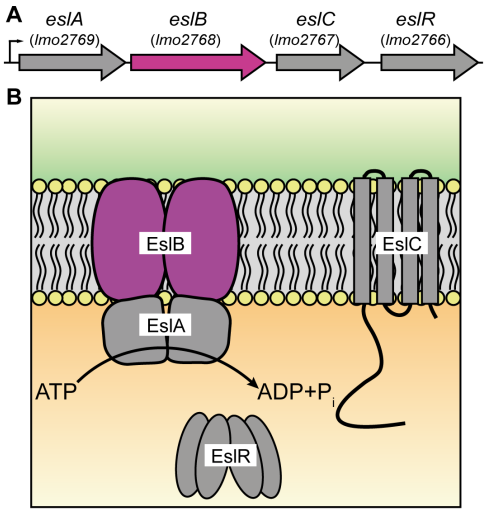

481

482

483 **Figure 1: Schematic representation of the *L. monocytogenes eslABCR* operon and cellular**
484 **location of the encoded proteins.** (A) Genomic arrangement of the *eslABCR* operon in *L.*
485 *monocytogenes*. Arrowheads indicate the orientation of the genes. Small black arrow indicates
486 the promoter identified in a previous study (Toledo-Arana et al., 2009). (B) Schematic of the
487 ABC transporter composed of the NBD protein EslA, which hydrolyses ATP, and the TMD
488 protein EslB, and the cytoplasmic RpiR family transcription regulator EslR. The membrane
489 topology of EslC, a protein of unknown function, was predicted using the TMHMM server 2.0
490 (Sonnhammer et al., 1998). The *eslB* gene and EslB protein, which were investigated as part
491 of the study, are highlighted in pink.

492

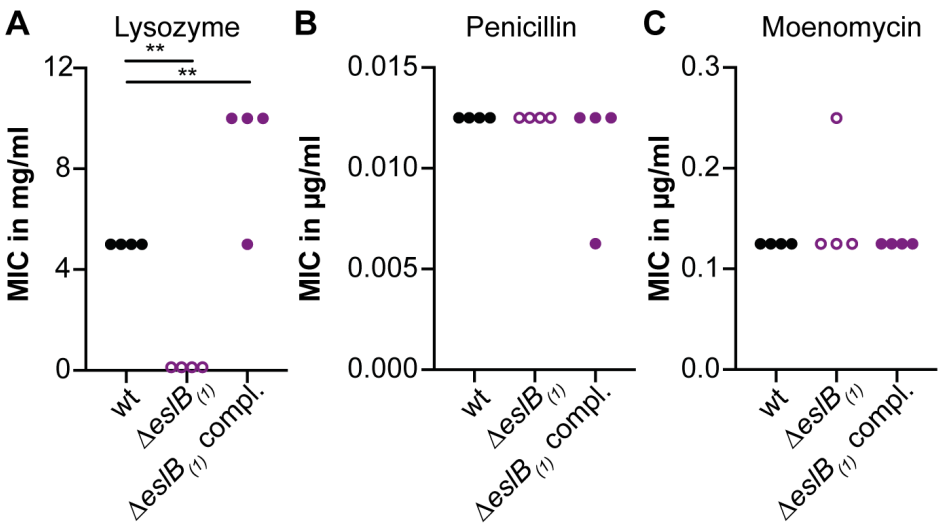

Figure 2: Impact of *eslB* deletion on resistance towards cell wall-targeting antimicrobials. (A-C) Minimal inhibitory concentration (MIC) of *L. monocytogenes* strains 10403S (wt), 10403SΔ*eslB*$_{(1)}$ and 10403SΔ*eslB*$_{(1)}$ compl. towards (A) lysozyme, (B) penicillin G and (C) moenomycin. Strain 10403SΔ*eslB*$_{(1)}$ compl. was grown in the presence of 1 mM IPTG. The results of four independent experiments are shown. For statistical analysis, a one-way ANOVA followed by a Dunnett's multiple comparisons test was used (** $p \leq 0.01$).

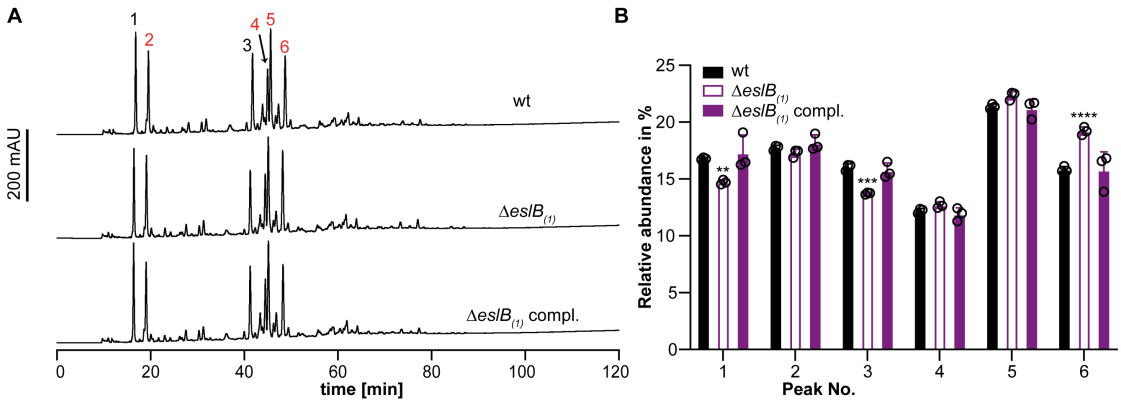

502
503
504 **Figure 3: Deletion of *eslB* leads to slight changes in the peptidoglycan structure.** (A) HPLC
505 analysis of muropeptides derived from mutanolysin digested peptidoglycan isolated from
506 strains 10403S (wt), 10403SΔ*eslB*$_{(1)}$ and 10403SΔ*eslB*$_{(1)}$ compl. (the latter grown in the
507 presence of 1 mM IPTG). The muropeptide spectrum of the wildtype strain 10403S has been
508 previously published (Rismondo et al., 2019) and was used again as part of this study as all
509 strains were analyzed at the same time. Major muropeptide peaks are numbered 1-6 according
510 to previously published HPLC spectra (Burke et al., 2014, Rismondo et al., 2015), with
511 numbers shown in red likely corresponding to muropeptides with N-deacetylated GlcNAc
512 residues and peaks 1-2 corresponding to monomeric and 4-6 to dimeric (crosslinked)
513 muropeptide fragments. (B) Quantification of the relative abundance of muropeptide peaks 1-
514 6 for peptidoglycan isolated of strains 10403S (wt), 10403SΔ*eslB*$_{(1)}$ and 10403SΔ*eslB*$_{(1)}$
515 compl.. For quantification, the sum of the peak areas was set to 100% and the area of individual
516 peaks was determined. Averages values and standard deviations were calculated from three
517 independent peptidoglycan extractions and plotted. For statistical analysis, a two-way ANOVA
518 followed by a Dunnett's multiple comparisons test was used (** $p \leq 0.01$, *** $p \leq 0.001$, ****
519 $p \leq 0.0001$).
520
521

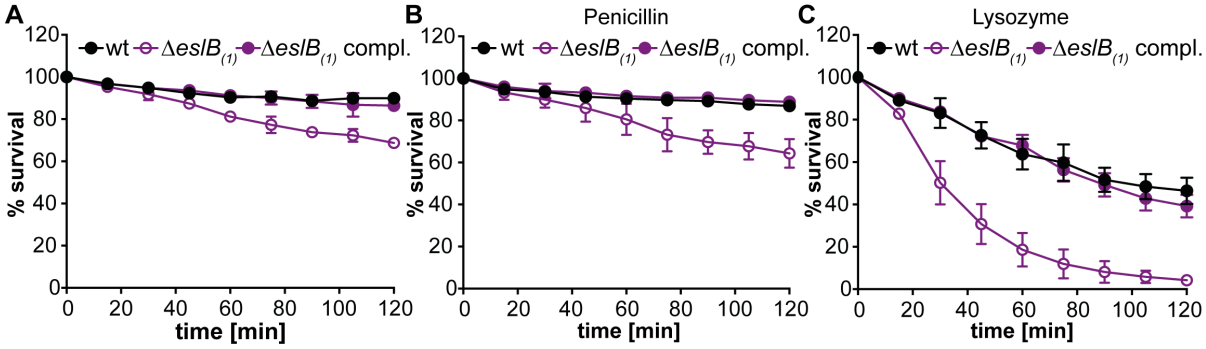

Figure 4: An *L. monocytogenes eslB* deletion strain shows increased endogenous and lysozyme-induced autolysis. Autolysis assays were performed with *L. monocytogenes* strains 10403S (wt), 10403SΔ*eslB*$_{(1)}$ and 10403SΔ*eslB*$_{(1)}$ compl.. Bacteria were grown for 4 h in BHI medium (containing 1 mM IPTG for 10403SΔ*eslB*$_{(1)}$ compl.) and subsequently bacterial suspensions prepared in (A) 50 mM Tris HCl pH 8, (B) 50 mM Tris HCl pH 8 containing 25 µg/ml penicillin, or (C) 50 mM Tris HCl pH 8 with 2.5 µg/ml lysozyme. Cell lysis was followed by taking OD_{600} readings every 15 min. The initial OD_{600} reading for each bacterial suspension was set to 100% and subsequent readings are shown as % of the initial OD_{600} reading. The average % OD_{600} values and standard deviations were calculated from three independent experiments and plotted.

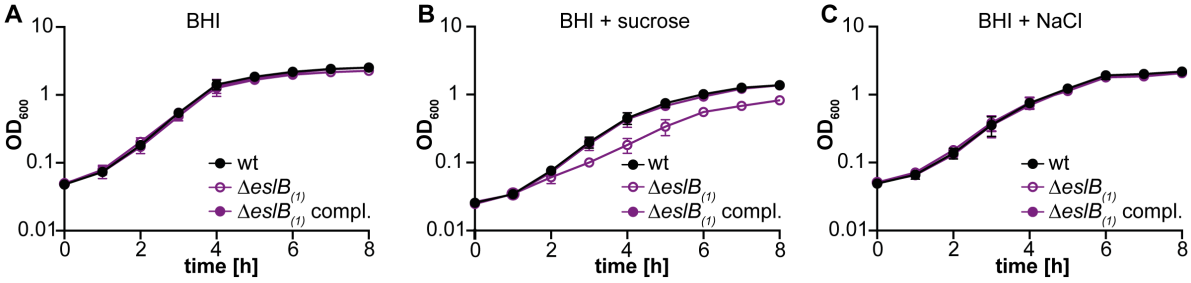

535

536

537 **Figure 5: Addition of sucrose but not NaCl negatively impacts the growth of the *L.***
538 ***monocytogenes eslB* mutant strain**. (A-C). Bacterial growth curves. *L. monocytogenes* strains
539 10403S (wt), 10403SΔ*eslB(1)* and 10403SΔ*eslB(1)* compl. were grown in (A) BHI broth, (B)
540 BHI broth containing 0.5 M sucrose or (C) BHI broth containing 0.5 M NaCl. Strain
541 10403SΔ*eslB(1)* compl. was grown in the presence of 1 mM IPTG. OD_{600} readings were
542 determined at hourly intervals and the average values and standard deviations from three
543 independent experiments calculated and plotted.

544

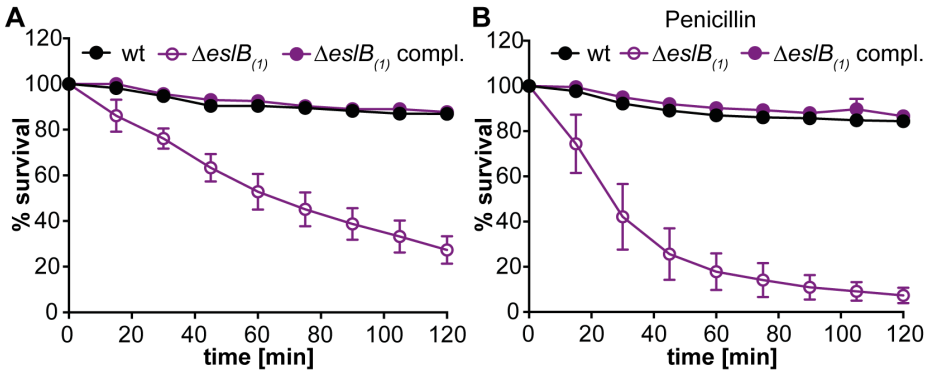

545

546

547 **Figure 6: Pre-growth in sucrose containing medium stimulates the endogenous and**
548 **penicillin-induced autolysis rate of an *L. monocytogenes eslB* mutant strain.** Autolysis
549 assays were performed with *L. monocytogenes* strains 10403S (wt), 10403SΔ*eslB*$_{(1)}$ and
550 10403SΔ*eslB*$_{(1)}$ compl.. Bacteria were grown for 4 h in BHI medium containing 0.5 M sucrose
551 (containing 1 mM IPTG for 10403SΔ*eslB*$_{(1)}$ compl.) and subsequently bacterial suspensions
552 prepared in (A) 50 mM Tris HCl pH 8, or (B) 50 mM Tris HCl pH 8 containing 25 µg/ml
553 penicillin. Cell lysis was followed by taking OD_{600} readings every 15 min. The initial OD_{600}
554 reading for each bacterial suspension was set to 100% and subsequent readings are shown as
555 % of the initial OD_{600} reading. The average % OD_{600} values and standard deviations were
556 calculated from three independent experiments and plotted.

557

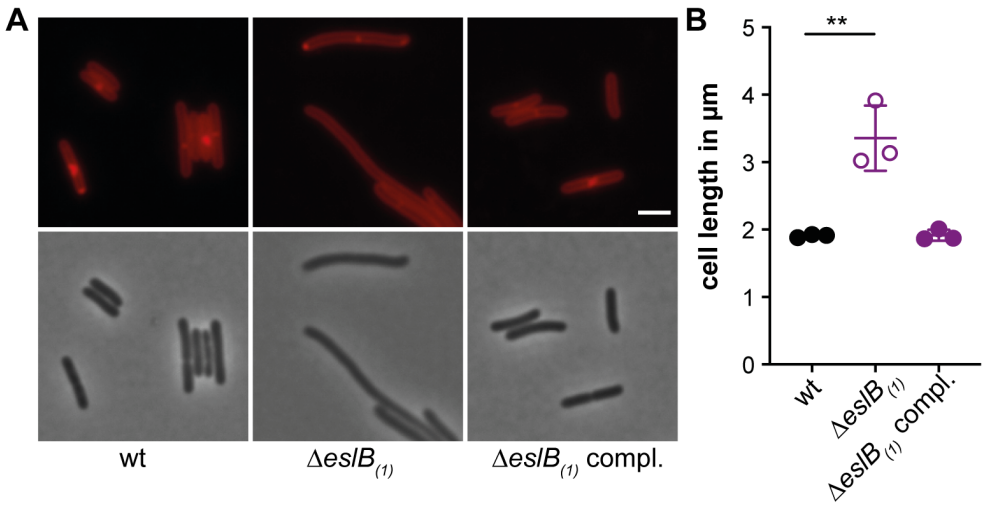

558

559

560 **Figure 7: The *L. monocytogenes eslB* mutant has a cell division defect and bacteria have**
561 **an increased cell length.** (A) Microscopy images of *L. monocytogenes* strains 10403S (wt),
562 10403SΔ*eslB*$_{(1)}$ and 10403SΔ*eslB*$_{(1)}$ compl.. Bacterial membranes were stained with nile red
563 and cells analyzed by phase contrast and fluorescence microscopy. Scale bar is 2 µm.
564 Representative images from three independent experiments are shown. (B) Cell length of *L.*
565 *monocytogenes* strains 10403S (wt), 10403SΔ*eslB*$_{(1)}$ and 10403SΔ*eslB*$_{(1)}$ compl.. The cell
566 length of 300 cells per strain was measured and the median cell length calculated. Three
567 independent experiments were performed, and the average values and standard deviation of the
568 median cell length plotted. For statistical analysis, a one-way ANOVA analysis followed by a
569 Dunnett's multiple comparisons test was used (** $p \leq 0.01$).

570

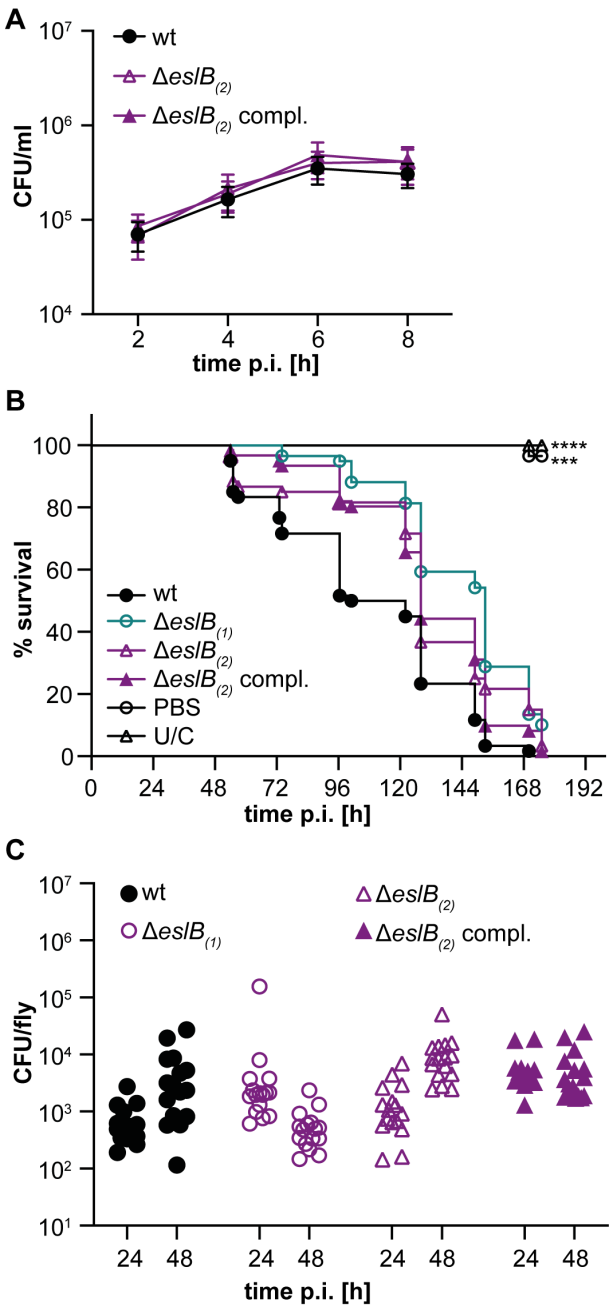

571

572

573 **Figure 8: Impact of the deletion of *eslB* on the virulence of *L. monocytogenes*.** (A)
574 Intracellular growth of *L. monocytogenes* strains 10403S (wt), 10403SΔ*eslB*$_{(2)}$ and
575 10403SΔ*eslB*$_{(2)}$ compl. in mouse bone marrow-derived macrophages (BMMs). For the
576 infection, bacteria were grown overnight at 30°C statically and used on the next day to infect
577 BMMs at an MOI of 2. The number of intracellular bacteria was determined 2, 4, 6 and 8 h
578 post infection as described in the methods section. Three technical repeats were performed per
579 experiment and strain and average values calculated. The average CFU count/ml and standard
580 deviations from three independent experiments were calculated and plotted. (B) Survival curve

581 of flies infected with *L. monocytogenes*. Flies were infected with *L. monocytogenes* strains
582 10403S (wt), 10403SΔ*eslB*$_{(1)}$, 10403SΔ*eslB*$_{(2)}$ and 10403SΔ*eslB*$_{(2)}$ compl.. Uninjected control
583 flies (U/C) and flies injected with PBS were used as controls. Fly death was monitored daily.
584 For statistical analysis, a one-way ANOVA followed by a Dunnett's multiple comparisons test
585 was used (*** $p \leq 0.001$, **** $p \leq 0.0001$). (C) Bacterial quantification. 16 flies infected with the
586 indicated *L. monocytogenes* strain were collected 24 and 48 h post infection and bacterial load
587 (CFU) determined as described in the methods section. For statistical analysis, a nested one-
588 way ANOVA followed by a Dunnett's multiple comparisons test was used. The observed
589 differences were not statistically significant.
590
591
592

593 **REFERENCES**

594 AUBRY, C., GOULARD, C., NAHORI, M. A., CAYET, N., DECALF, J., SACHSE, M., BONECA, I. G.,
595 COSSART, P. & DUSSURGET, O. 2011. OatA, a peptidoglycan O-acetyltransferase
596 involved in *Listeria monocytogenes* immune escape, is critical for virulence. *J Infect*
597 *Dis,* 204**,** 731-40.
598 BENACHOUR, A., LADJOUZI, R., LE JEUNE, A., HÉBERT, L., THORPE, S., COURTIN, P., CHAPOT-
599 CHARTIER, M. P., PRAJSNAR, T. K., FOSTER, S. J. & MESNAGE, S. 2012. The lysozyme-
600 induced peptidoglycan N-acetylglucosamine deacetylase PgdA (EF1843) is required
601 for *Enterococcus faecalis* virulence. *J Bacteriol,* 194**,** 6066-73.
602 BERA, A., BISWAS, R., HERBERT, S., KULAUZOVIC, E., WEIDENMAIER, C., PESCHEL, A. & GÖTZ,
603 F. 2007. Influence of wall teichoic acid on lysozyme resistance in *Staphylococcus*
604 *aureus*. *J Bacteriol,* 189**,** 280-3.
605 BERA, A., HERBERT, S., JAKOB, A., VOLLMER, W. & GÖTZ, F. 2005. Why are pathogenic
606 staphylococci so lysozyme resistant? The peptidoglycan O-acetyltransferase OatA is
607 the major determinant for lysozyme resistance of *Staphylococcus aureus*. *Mol*
608 *Microbiol,* 55**,** 778-87.
609 BERNTSSON, R. P., SMITS, S. H., SCHMITT, L., SLOTBOOM, D. J. & POOLMAN, B. 2010. A
610 structural classification of substrate-binding proteins. *FEBS Lett,* 584**,** 2606-17.
611 BIERNE, H., SABET, C., PERSONNIC, N. & COSSART, P. 2007. Internalins: a complex family of
612 leucine-rich repeat-containing proteins in *Listeria monocytogenes*. *Microbes Infect,* 9**,**
613 1156-66.
614 BONECA, I. G., DUSSURGET, O., CABANES, D., NAHORI, M. A., SOUSA, S., LECUIT, M.,
615 PSYLINAKIS, E., BOURIOTIS, V., HUGOT, J. P., GIOVANNINI, M., COYLE, A., BERTIN, J.,
616 NAMANE, A., ROUSSELLE, J. C., CAYET, N., PREVOST, M. C., BALLOY, V., CHIGNARD, M.,
617 PHILPOTT, D. J., COSSART, P. & GIRARDIN, S. E. 2007. A critical role for peptidoglycan
618 N-deacetylation in *Listeria* evasion from the host innate immune system. *Proc Natl*
619 *Acad Sci U S A,* 104**,** 997-1002.
620 BURKE, T. P., LOUKITCHEVA, A., ZEMANSKY, J., WHEELER, R., BONECA, I. G. & PORTNOY, D. A.
621 2014. *Listeria monocytogenes* is resistant to lysozyme through the regulation, not the
622 acquisition, of cell wall-modifying enzymes. *J Bacteriol,* 196**,** 3756-67.
623 CALLEWAERT, L. & MICHIELS, C. W. 2010. Lysozymes in the animal kingdom. *J Biosci,* 35**,** 127-
624 60.
625 CAMILLI, A., TILNEY, L. G. & PORTNOY, D. A. 1993. Dual roles of *plcA* in *Listeria monocytogenes*
626 pathogenesis. *Mol Microbiol,* 8**,** 143-57.
627 CARROLL, S. A., HAIN, T., TECHNOW, U., DARJI, A., PASHALIDIS, P., JOSEPH, S. W. &
628 CHAKRABORTY, T. 2003. Identification and characterization of a peptidoglycan
629 hydrolase, MurA, of *Listeria monocytogenes*, a muramidase needed for cell
630 separation. *J Bacteriol,* 185**,** 6801-8.
631 CORRIGAN, R. M., ABBOTT, J. C., BURHENNE, H., KAEVER, V. & GRÜNDLING, A. 2011. c-di-AMP
632 is a new second messenger in *Staphylococcus aureus* with a role in controlling cell size
633 and envelope stress. *PLoS Pathog,* 7**,** e1002217.
634 DAFFRE, S., KYLSTEN, P., SAMAKOVLIS, C. & HULTMARK, D. 1994. The lysozyme locus in
635 Drosophila melanogaster: an expanded gene family adapted for expression in the
636 digestive tract. *Mol Gen Genet,* 242**,** 152-62.
637 DAHL, U., JAEGER, T., NGUYEN, B. T., SATTLER, J. M. & MAYER, C. 2004. Identification of a
638 phosphotransferase system of *Escherichia coli* required for growth on N-
639 acetylmuramic acid. *J Bacteriol,* 186**,** 2385-92.

640 DAVIDSON, A. L., DASSA, E., ORELLE, C. & CHEN, J. 2008. Structure, function, and evolution of
641 bacterial ATP-binding cassette systems. *Microbiol Mol Biol Rev,* 72**,** 317-64, table of
642 contents.
643 DAWSON, R. J. & LOCHER, K. P. 2006. Structure of a bacterial multidrug ABC transporter.
644 *Nature,* 443**,** 180-5.
645 DE JONGE, B. L., CHANG, Y. S., GAGE, D. & TOMASZ, A. 1992. Peptidoglycan composition of a
646 highly methicillin-resistant *Staphylococcus aureus* strain. The role of penicillin binding
647 protein 2A. *J Biol Chem,* 267**,** 11248-54.
648 DURACK, J., BURKE, T. P. & PORTNOY, D. A. 2015. A prl mutation in SecY suppresses secretion
649 and virulence defects of *Listeria monocytogenes secA2* mutants. *J Bacteriol,* 197**,** 932-
650 42.
651 GAILLARD, J. L., BERCHE, P., FREHEL, C., GOUIN, E. & COSSART, P. 1991. Entry of *L.*
652 *monocytogenes* into cells is mediated by internalin, a repeat protein reminiscent of
653 surface antigens from gram-positive cocci. *Cell,* 65**,** 1127-41.
654 HÉBERT, L., COURTIN, P., TORELLI, R., SANGUINETTI, M., CHAPOT-CHARTIER, M. P., AUFFRAY,
655 Y. & BENACHOUR, A. 2007. *Enterococcus faecalis* constitutes an unusual bacterial
656 model in lysozyme resistance. *Infect Immun,* 75**,** 5390-8.
657 HERBERT, S., BERA, A., NERZ, C., KRAUS, D., PESCHEL, A., GOERKE, C., MEEHL, M., CHEUNG, A.
658 & GOTZ, F. 2007. Molecular basis of resistance to muramidase and cationic
659 antimicrobial peptide activity of lysozyme in staphylococci. *PLoS Pathog,* 3**,** e102.
660 HIGGINS, C. F. 1992. ABC transporters: from microorganisms to man. *Annu Rev Cell Biol,* 8**,**
661 67-113.
662 HÖLTJE, J. V. 1998. Growth of the stress-bearing and shape-maintaining murein sacculus of
663 *Escherichia coli*. *Microbiol Mol Biol Rev,* 62**,** 181-203.
664 HUBER, G. & NESEMANN, G. 1968. Moenomycin, an inhibitor of cell wall synthesis. *Biochem*
665 *Biophys Res Commun,* 30**,** 7-13.
666 IBRAHIM, H. R., AOKI, T. & PELLEGRINI, A. 2002. Strategies for new antimicrobial proteins and
667 peptides: lysozyme and aprotinin as model molecules. *Curr Pharm Des,* 8**,** 671-93.
668 JAEGER, T. & MAYER, C. 2008. The transcriptional factors MurR and catabolite activator
669 protein regulate N-acetylmuramic acid catabolism in *Escherichia coli*. *J Bacteriol,* 190**,**
670 6598-608.
671 KIM, C., SONG, S. & PARK, C. 1997. The D-allose operon of *Escherichia coli* K-12. *J Bacteriol,*
672 179**,** 7631-7.
673 KOCH, A. L. 2003. Bacterial wall as target for attack: past, present, and future research. *Clin*
674 *Microbiol Rev,* 16**,** 673-87.
675 LAUER, P., CHOW, M. Y., LOESSNER, M. J., PORTNOY, D. A. & CALENDAR, R. 2002.
676 Construction, characterization, and use of two *Listeria monocytogenes* site-specific
677 phage integration vectors. *J Bacteriol,* 184**,** 4177-86.
678 LE JEUNE, A., TORELLI, R., SANGUINETTI, M., GIARD, J. C., HARTKE, A., AUFFRAY, Y. &
679 BENACHOUR, A. 2010. The extracytoplasmic function sigma factor SigV plays a key role
680 in the original model of lysozyme resistance and virulence of *Enterococcus faecalis*.
681 *PLoS One,* 5**,** e9658.
682 LOCHER, K. P. 2016. Mechanistic diversity in ATP-binding cassette (ABC) transporters. *Nat*
683 *Struct Mol Biol,* 23**,** 487-93.
684 MÄCHTEL, R., NARDUCCI, A., GRIFFITH, D. A., CORDES, T. & ORELLE, C. 2019. An integrated
685 transport mechanism of the maltose ABC importer. *Res Microbiol,* 170**,** 321-337.

686 PILGRIM, S., KOLB-MAURER, A., GENTSCHEV, I., GOEBEL, W. & KUHN, M. 2003. Deletion of
687 the gene encoding p60 in *Listeria monocytogenes* leads to abnormal cell division and
688 loss of actin-based motility. *Infect Immun,* 71**,** 3473-84.
689 POULSEN, T. S., CHANG, Y. Y. & HOVE-JENSEN, B. 1999. D-Allose catabolism of *Escherichia col*i:
690 involvement of alsI and regulation of als regulon expression by allose and ribose. *J*
691 *Bacteriol,* 181**,** 7126-30.
692 RAE, C. S., GEISSLER, A., ADAMSON, P. C. & PORTNOY, D. A. 2011. Mutations of the *Listeria*
693 *monocytogenes* peptidoglycan N-deacetylase and O-acetylase result in enhanced
694 lysozyme sensitivity, bacteriolysis, and hyperinduction of innate immune pathways.
695 *Infect Immun,* 79**,** 3596-606.
696 RISMONDO, J., HALBEDEL, S. & GRÜNDLING, A. 2019. Cell Shape and Antibiotic Resistance Are
697 Maintained by the Activity of Multiple FtsW and RodA Enzymes in *Listeria*
698 *monocytogenes*. *MBio,* 10.
699 RISMONDO, J., MOLLER, L., ALDRIDGE, C., GRAY, J., VOLLMER, W. & HALBEDEL, S. 2015.
700 Discrete and overlapping functions of peptidoglycan synthases in growth, cell division
701 and virulence of *Listeria monocytogenes*. *Mol Microbiol,* 95**,** 332-51.
702 SARKAR, P., YARLAGADDA, V., GHOSH, C. & HALDAR, J. 2017. A review on cell wall synthesis
703 inhibitors with an emphasis on glycopeptide antibiotics. *Medchemcomm,* 8**,** 516-533.
704 SAUVAGE, E. & TERRAK, M. 2016. Glycosyltransferases and Transpeptidases/Penicillin-
705 Binding Proteins: Valuable Targets for New Antibacterials. *Antibiotics (Basel),* 5.
706 SHARROCK, J., ESTACIO-GOMEZ, A., JACOBSON, J., KIERDORF, K., SOUTHALL, T. D. & DIONNE,
707 M. S. 2019. *fs(1)h* controls metabolic and immune function and enhances survival via
708 AKT and FOXO in *Drosophila*. *Dis Model Mech,* 12.
709 SLOTBOOM, D. J. 2014. Structural and mechanistic insights into prokaryotic energy-coupling
710 factor transporters. *Nat Rev Microbiol,* 12**,** 79-87.
711 SONNHAMMER, E. L., VON HEIJNE, G. & KROGH, A. 1998. A hidden Markov model for
712 predicting transmembrane helices in protein sequences. *Proc Int Conf Intell Syst Mol*
713 *Biol,* 6**,** 175-82.
714 SORENSEN, K. I. & HOVE-JENSEN, B. 1996. Ribose catabolism of *Escherichia coli*:
715 characterization of the *rpiB* gene encoding ribose phosphate isomerase B and of the
716 *rpiR* gene, which is involved in regulation of *rpiB* expression. *J Bacteriol,* 178**,** 1003-11.
717 STAPELS, D. A. C., HILL, P. W. S., WESTERMANN, A. J., FISHER, R. A., THURSTON, T. L., SALIBA,
718 A. E., BLOMMESTEIN, I., VOGEL, J. & HELAINE, S. 2018. *Salmonella* persisters
719 undermine host immune defenses during antibiotic treatment. *Science,* 362**,** 1156-
720 1160.
721 TANAKA, K. J., SONG, S., MASON, K. & PINKETT, H. W. 2018. Selective substrate uptake: The
722 role of ATP-binding cassette (ABC) importers in pathogenesis. *Biochim Biophys Acta*
723 *Biomembr,* 1860**,** 868-877.
724 TIPPER, D. J. & STROMINGER, J. L. 1965. Mechanism of action of penicillins: a proposal based
725 on their structural similarity to acyl-D-alanyl-D-alanine. *Proc Natl Acad Sci U S A,* 54**,**
726 1133-41.
727 TOLEDO-ARANA, A., DUSSURGET, O., NIKITAS, G., SESTO, N., GUET-REVILLET, H., BALESTRINO,
728 D., LOH, E., GRIPENLAND, J., TIENSUU, T., VAITKEVICIUS, K., BARTHELEMY, M.,
729 VERGASSOLA, M., NAHORI, M. A., SOUBIGOU, G., REGNAULT, B., COPPEE, J. Y., LECUIT,
730 M., JOHANSSON, J. & COSSART, P. 2009. The *Listeria* transcriptional landscape from
731 saprophytism to virulence. *Nature,* 459**,** 950-6.

732 VAN HEIJENOORT, J. 2001. Formation of the glycan chains in the synthesis of bacterial
733 peptidoglycan. *Glycobiology,* 11**,** 25R-36R.
734 VOLLMER, W. & TOMASZ, A. 2000. The *pgdA* gene encodes for a peptidoglycan N-
735 acetylglucosamine deacetylase in *Streptococcus pneumoniae*. *J Biol Chem,* 275**,** 20496-
736 501.
737 YAMAMOTO, H., SERIZAWA, M., THOMPSON, J. & SEKIGUCHI, J. 2001. Regulation of the *glv*
738 operon in *Bacillus subtilis*: YfiA (GlvR) is a positive regulator of the operon that is
739 repressed through CcpA and cre. *J Bacteriol,* 183**,** 5110-21.
740